Ecological Indicators 142 (2022) 109162

Contents lists available at ScienceDirect

Ecological Indicators

journal homepage: www.elsevier.com/locate/ecolind

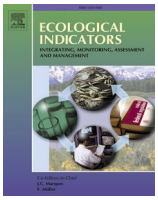

Optimizing the airborne laser scanning estimation of basal area larger than mean (*BALM*): An indicator of cohort balance in forests

Syed Adnan [a,*], Rubén Valbuena [b,c], Tuomo Kauranne [d], Ranjith Gopalakrishnan [a], Matti Maltamo [a]

[a] University of Eastern Finland, School of Forest Sciences, P.O. Box 111, FI-80101 Joensuu, Finland
[b] Swedish University of Agricultural Sciences, SLU Skogsmarksgränd 17, SE-901 83 Umeå, Sweden
[c] Bangor University, School of Natural Sciences, Thoday Building, Bangor, Gwynedd LL57 2UW, UK
[d] Arbonaut Ltd., Kaislakatu 2, FI-80130 Joensuu, Finland

ARTICLE INFO

Keywords:
Forest structure
LiDAR
Plot size effect
Sample size effect
Point density effect
Airborne laser scanning

ABSTRACT

Airborne laser scanning (ALS) assisted basal area larger than mean (*BALM*) estimation measures the cohort balance in forests and provides adequate opportunities to describe forest structure. However, a problem still exists that how the plot size, sample size (number of trees), and ALS point density affect the *BALM* estimation. We tackled this question by using both field and ALS data from a typical managed boreal forest area in Finland. Various concentric circular plots (1–15 m radii) were simulated within the actual field plots (squared) and the optimal plot size and sample size were selected by observing changes in the absolute correlation between *BALM* estimates and various ALS metrics. Instability in the correlation was found at the smaller concentric circular plots (1–5 m radii) and sample sizes (less than 6 trees) but as the plot size and sample size increased, the correlation followed a convex curve. The maximum correlation was found between a concentric circular plot size 11–14 m radii (380–615 m^2 area) and sample size 50–80 trees which could be the optimal plot size and sample size for a reliable *BALM* estimation. With regards to the ALS point density, no major effects were observed on the relationship between *BALM* estimates and various ALS metrics unless the point density is less than at least 5 points m^{-2}. The point density of the current nationwide ALS survey is matching the minimum point density requirement obtained in this study and thus it is suitable for a reliable forest structural assessment.

1. Introduction

Forest attributes prediction from airborne laser scanning (ALS) is becoming more common and is increasingly being adopted for forest inventory. The main reasons for this are the considerable improvements in the accuracy of height estimation, spatial coverage, and timeliness of the ALS data (Maltamo et al., 2018; Almeida et al., 2019; Hauglin et al., 2021). ALS based inventories are now a standard part of forest measurement operations in several countries (Hollaus et al., 2009; Maltamo et al., 2014). In an ALS-based system, an onboard lidar detection and ranging (LIDAR) sensor is used to scan a forest from an aeroplane. The LIDAR sensor measures distances by emitting laser pulses and detecting the backscattered echoes, precisely computes the height and location of reflecting objects, and produces a detailed 3D point cloud of the forest canopy (Maltamo et al., 2005; Gaveau and Hill, 2003; Davenport et al., 2004). This ALS-based 3D point cloud provides valuable information about forest vertical structures and is considered as highly effective and useful data for regional monitoring than the other remote sensing approaches (Maltamo et al., 2006). ALS derived metrics describe salient forest characteristics and are used to study various forest attributes including volume (Naesset, 1997), diameter at breast height (*dbh*) and vertical profiles (Maltamo et al., 2004), tree species and competition (Suratno et al., 2009; Pedersen et al., 2012), spatial patterns of trees (Pippuri et al., 2012), wildlife habitat modelling (Melin et al., 2013), forest structure (Valbuena et al., 2013; Adnan et al., 2017), stand age (Maltamo et al., 2020), and aboveground biomass and carbon stocks (Coomes et al., 2018; Adnan et al., 2021).

The prediction of forest attributes from ALS can be accomplished by two approaches (Maltamo et al., 2014). First, the individual tree detection approach wherein the treetops are detected and then

* Corresponding author.
E-mail addresses: adnan@uef.fi (S. Adnan), ruben.valbuena@slu.se (R. Valbuena), tuomo.kauranne@arbonaut.com (T. Kauranne), ranjith.gopalakrishnan@uef.fi (R. Gopalakrishnan), matti.maltamo@uef.fi (M. Maltamo).

https://doi.org/10.1016/j.ecolind.2022.109162
Received 10 March 2022; Received in revised form 23 June 2022; Accepted 10 July 2022
Available online 21 July 2022

allometric models are used to extract features and measure the desired forest attributes (Kaartinen et al., 2012). Second is the area-based approach in which ALS metrics derived from a given field plot (predictor variables) are linked with the desired forest attribute (response variable) from the same field plot (Packalén and Maltamo, 2006; Adnan et al., 2019). The accuracy of the predicted forest attributes and cost of LIDAR surveys depends on various ALS parameters such as platform altitude (Goodwin et al., 2006), maximum scan angle (Holmgren et al., 2003), and ALS point density (points m^{-2}) (Næsset and Økland, 2002; Maltamo et al., 2006; Adnan et al., 2017). According to Næsset and Økland (2002), for accurate estimation of individual crown attributes in Scot pines (*Pinus sylvestris* L.) and Norway spruce (*Picea abies* (L.) Karst.) forests, an average point spacing of fewer than 1 m is not sufficient. In the context of volume estimation, the effect of ALS point density is very marginal (Maltamo et al., 2006). Similar results have been presented by Adnan et al. (2017) that any point density higher than at least 3 points m^{-2} is suitable for the accurate prediction of different forest structural types based on the Gini coefficient of tree size inequality. This study tackles the issue of the point density effect on the relationship between the basal area larger than mean (*BALM*) and ALS metrics.

Basal area larger than mean (or basal area larger than the quadratic mean stand diameter) is a useful forest structural indicator that measures the cohort balance in forests but has often been ignored by forest scientists. Gove (2004) first highlighted its usefulness in stocking guides which is a process of decision-making about silvicultural activities. *BALM* is easy to calculate from any forest inventory data as it is the accumulated basal areas of all standing trees with $dbh \geq D_{QMD}$ in a plot (Fig. 1) or it can also be calculated from diameter frequency or basal area-size distribution (Gove and Patil, 1998). According to Gove (2004), the most appropriate quantity is the proportional *BALM* as given in Eq. (1).

$$BALM = \frac{\sum_{dbh \geq D_{QMD}} \pi \left(\frac{dbh}{2}\right)^2}{B}, \quad (1)$$

where *dbh* is the tree diameter at breast height, D_{QMD} is the quadratic mean diameter and *B* is the total basal area of a plot.

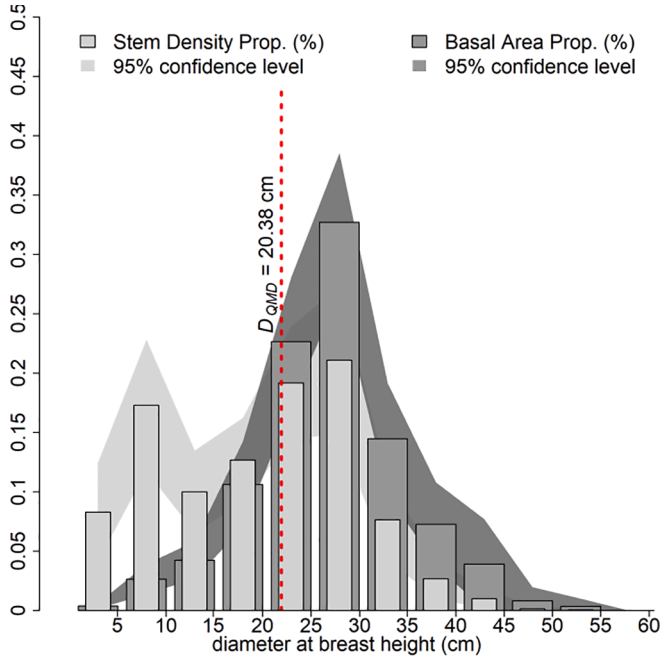

Fig. 1. Graphical illustration of the Basal Area Larger than Mean (*BALM*). The light grey bars represent the stem density proportion (diameter distribution), and the dark grey bars show their corresponding proportion of the basal area. *BALM* is the proportion of accumulated basal areas of all trees whose $dbh > D_{QMD}$ (quadratic mean diameter; red vertical dotted line) (Gove, 2004).

BALM represents the skewness of tree diameter distribution and lower values of *BALM* denote the open canopies, for example, reversed-J type forest structures while higher values represent closed canopies dominated by mature trees (Valbuena, 2015). It is useful for evaluating the relative dominance of different tree layers, biomass stocking in one or many tree layers, or ecology of species whether they prefer single layer or multi-layers tree structures (Mononen et al., 2018). In growth modelling, *BALM* may have positive effects on the shade-tolerant species as they are able to grow in the understory vegetation but the shade-intolerant species are negatively affected because the stand becomes more crowded, they may experience more shaded conditions and their rate of growth may decrease (Lessard et al., 2001; Oboite and Comeau, 2019). Valbuena et al. (2013) also characterized different forest structural types from ALS data and suggested that the proportion of basal area (*BALM*) and the Gini coefficient of tree size inequality are the two potential independent bivariate descriptors that could be used to fully describe different forest structures and indicate symmetric or asymmetric competition. Adnan et al. (2019) also applied *BALM* together with other forest attributes (Gini coefficient of tree size inequality, stand density and D_{QMD}) and performed a bioregional forest structural type assessment. However, due to the diverse sizes of field plots in their bioregional sites, they noticed that the size of the plot could influence the estimation of their forest attributes. The stand density and D_{QMD} and how the plot size influences these attributes are well studied (Gray, 2003; Ruiz et al., 2014; Häbel et al., 2019) and the plot size effect on the values of the Gini coefficient of tree size inequality has been evaluated in Adnan et al. (2017). However, the effect of plot size (and sample size) on the relationship between *BALM* values and ALS metrics or an ALS-assisted optimal plot size and sample size selection for a reliable *BALM* estimation is still missing in the scientific literature.

In national forest inventories (NFI), the purpose of an optimal plot size is to obtain results with the highest possible accuracy within a given fixed budget or a desired precise result at the lowest cost (Päivinen, 1987). However, the selection of the optimal plot size also relies mainly on the variable of interest, the purpose of forest inventory, and other factors, for example, time, field measurements, and inconsistency of variables between plots (Henttonen and Kangas, 2015). As the size of a plot increases, its effect on the estimated forest attributes decreases (Barbeito et al., 2009). A smaller plot size has a negative effect on the stem diameter distribution accuracy estimated from ALS (Maltamo et al., 2019) while a larger plot size will increase the budget, time, and data collection efforts (Chytrý and Otýpková, 2003). Similarly, on some of the forest attributes such as biomass and volume, the larger plot sizes will pose an averaging effect (Gobakken and Næsset, 2008; Ruiz et al., 2014), while on other forest attributes this averaging effect is not applicable, for example, forest structure and species richness (Coomes and Allen, 2007). In fact, if the plot size increases, the forest structural diversity and species richness also increase (Otypková and Chytry, 2006). Thus, changing the observation scale could alter the estimation of any forest attribute including *BALM*, and if the size of a plot increases, the estimation of *BALM* could become more stable, but essentially the condition of different stands would aggregate (Coomes and Allen, 2007). It is also a challenging task in spatial statistics to interpret the data analysed at different scales (Gotway and Young, 2002). Therefore, optimal plot size is necessary for any forest attribute including *BALM* which should be large enough to obtain stable and reliable results but not larger than the required size due to the time, cost, and data collection efforts involved.

In this study, we focus on the ALS assisted estimation of *BALM* which is an important forest structural indicator that can be used to measure the cohort balance in forests and separate various forest structural types. We address how the plot size, sample size, and point density of ALS data affect the relationship between *BALM* estimates and ALS metrics. We aim to select an optimal plot size for a reliable *BALM* estimation in the boreal forest and postulate that the effect of plot size would be dominant

as compared to the stand density and point density of ALS metrics. The developed methodology in this study is simple, based on simulations, and can easily be replicated in any forest area.

2. Material and methods

2.1. Study area and data collection

This study was conducted in Kiihtelysvaara inventory area located in the eastern Finland (62°31′N, 30°10′E) (Fig. 2). The area is a typical managed boreal forest dominated by Scot pine (*Pinus sylvestris* L.) and Norway spruce (*Picea abies* (L.) Karst.) which cover 73 % and 16 % of the wood volume, respectively. Deciduous species such as downy birch (*Betula pubescens* Ehrh.) and silver birch (*B. pendula* Roth.) represent the remaining 11 % of wood volume (Packalén et al., 2013). The proportion of such managed forests in Finland is 87.4 % (approximately 20.1 million hectares). In 2010, a field campaign was carried out from May to June, and data was collected in 79 square-shaped field plots (hereafter actual field plots) of various dimensions (20 × 20, 25 × 25, 30 × 30, the larger ones in sparse stand density areas). The forest stands were selected using stratified random sampling to represent both homogeneous even-sized areas and heterogeneous forest structures. Within the stands, the field plots were purposively selected at representative areas to avoid plots located at the stand borders, high cost, and efforts to measure all individual trees within the plot. The absolute position (longitude : X_{true} and latitude : Y_{true}) of all individual trees with $dbh > 5$ cm and height greater than 4 m were recorded from high-resolution ALS data using the individual tree detection method (Packalén et al., 2013). The locations were then verified in the field and *dbh* measurements were collected. The minimum, mean, and maximum stand density (N), D_{QMD} and basal area in the study area are 467, 1298, and 3025 trees ha^{-1}, 10, 17 and 29 cm and, 14, 25 and 44 m^2 ha^{-1}, respectively (Adnan et al., 2017).

2.2. Designing concentric circular plots and minimum number of simulations within the actual field plots

For the concentric circular plots design, the initial tasks were to convert the true coordinates (X_{true}, Y_{true}) of all trees into relative coordinates, edge correction, and sensitivity analysis to select the minimum number of simulations. And then, within each actual field plot, concentric circular plots (with radius varying from 1 to 15 m, with 1 m increments) were simulated at random positions. As the coordinates and *dbh* of all trees were available, we computed the *BALM* from the trees *dbh* within each concentric circular plot. Similarly, the ALS data could also be extracted using the coordinates of the concentric circular plots and can later be used to compute metrics commonly used in the area-based approach (Packalén and Maltamo, 2006).

For the conversion of true coordinates into relative coordinates, plot rotation and translation are required (Adnan et al., 2017). However, there was no need for the plot rotation because the edges of actual field plots were coinciding with the UTM grid in the study area. For plot translation, the origin of axes (0,0) was assigned to the southwest corner of the actual field plot to convert the true coordinates into relative coordinates. The relative coordinates ($X_{relative}$, $Y_{relative}$) were then obtained by subtracting the true coordinates of the southwest corner (X_{SW}, Y_{SW}) from the true coordinates (X_{true}, Y_{true}) of each individual tree.

$$(X_{relative}, Y_{relative}) = (X_{true}, Y_{true}) - (X_{SW}, Y_{SW}) \quad (2)$$

The next step was the edge correction method because ignoring the immediate neighbours outside the boundary could produce biased statistical results (Pommerening and Stoyan, 2006). In this study, the periodic edge correction method was applied to reduce this bias because Pommerening and Stoyan (2006) found it better than the other alternatives. It consists of replicating the same spatial pattern of trees around the actual field plot. Thus, concentric circular plots randomly positioned at the edge would also include trees located outside the boundary of the actual field plot (Fig. 3).

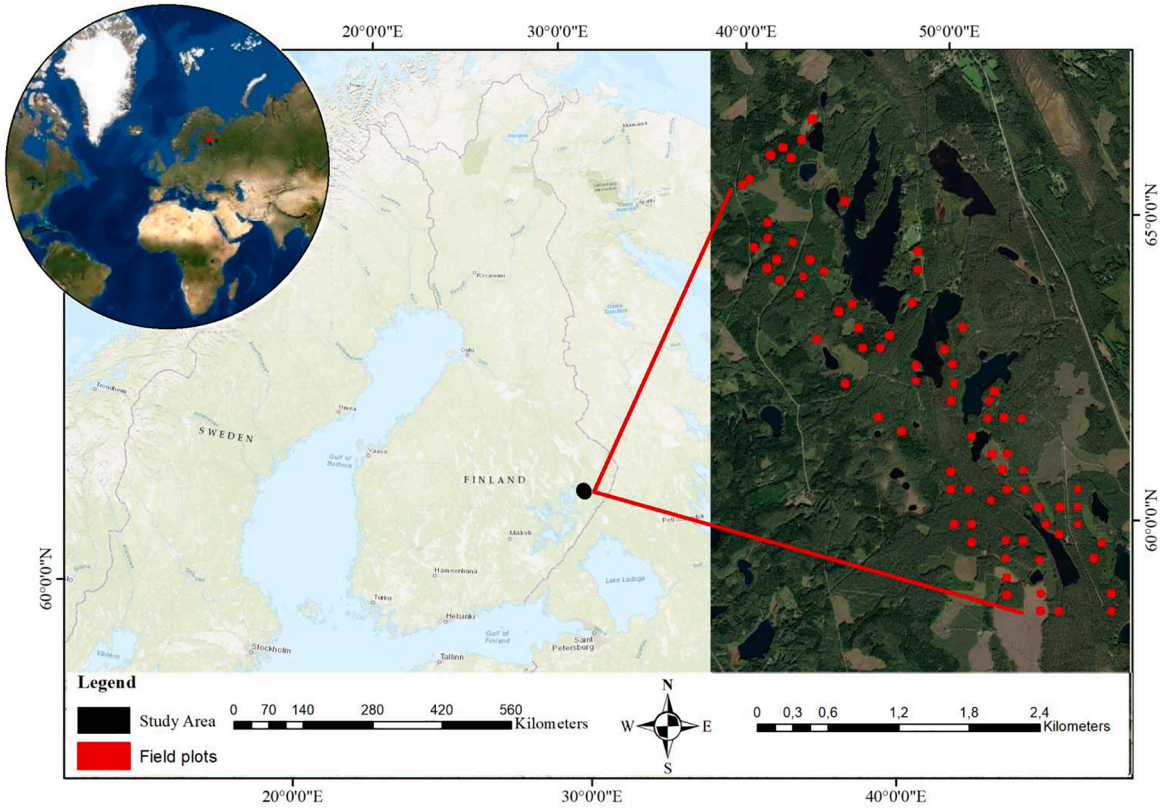

Fig. 2. Map showing the study area (Kiihtelysvaara inventory area) and the actual field plots located in Eastern Finland (background base maps © Esri).

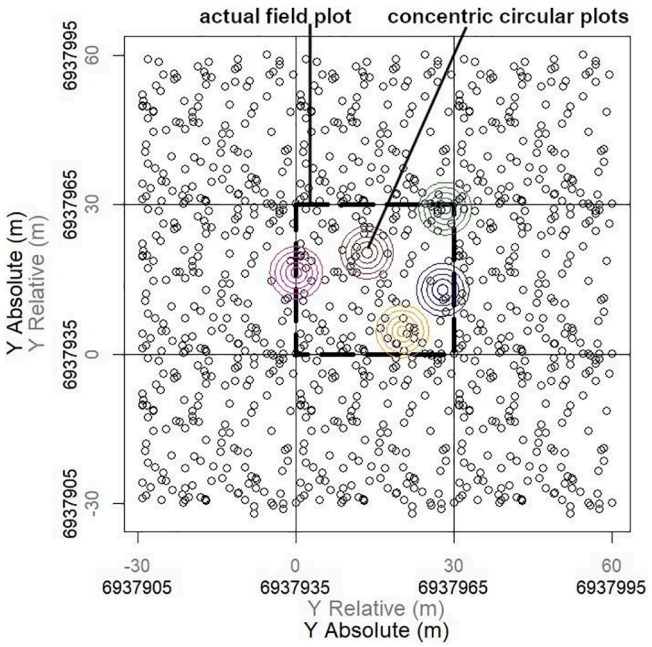

Fig. 3. Simulation of concentric circular plots (1–5 m radius) at five random positions (for simplicity) within the actual field plot represented by the dashed line in the centre and surrounded by a periodic boundary (edge correction method). The dots represent the tree positions within the actual field plot.

In the final step, a sensitivity analysis was applied to select minimum numbers of simulations (k) that could produce stable and robust *BALM* estimation. We randomly selected an actual field plot and applied different numbers of simulations (10, 50, 100, 500, 700, and 1000), and in every single simulation, a random position (X_{sim}, Y_{sim}) was selected and *BALM* was computed in concentric circular plots ranging from 1 to 15 m radii. This process was repeated for all k number of simulations. Then, the mean of those *BALM* values ($\overline{BALM}$) and standard error of mean (SEM) were calculated for each concentric circular plot.

$$SEM = \sigma/\sqrt{m}, \tag{3}$$

where σ is the standard deviation and m the sample size.

SEM which measures the variability of $\overline{BALM}$ was used to fix the minimum numbers of simulations k that could produce stable *BALM* estimation. Any further increase in simulations would not considerably improve the results. After selecting the minimum number of simulations (k) using the sensitivity analysis, the process was repeated for all the remaining actual field plots. The random position of each simulation (X_{sim}, Y_{sim}) was later used to extract the corresponding ALS data of the concentric circular plots.

2.3. Comparing the BALM estimations

To compare the *BALM* estimations, a graph was constructed that compared the $\overline{BALM}$ values for increasing concentric circular plot size s in all actual field plots. As the size s of the concentric circular plot increases, the *BALM* value within must approach the value of the entire actual field plot (Adnan et al., 2017). Thus, *BALM* value of the entire actual field plot was used as a reference ($BALM_{ref}$) (Zhang et al., 2022). The $\overline{BALM}$ value of each concentric circular plot was then subtracted from the $BALM_{ref}$ to get the absolute *BALM* difference ($\overline{BALM}_{diff}$). This way it was possible to analyse the differences and directly compare all *BALM* results.

$$\overline{BALM}_{diff} = |\overline{BALM} - BALM_{ref}| \tag{4}$$

2.4. ALS data collection and processing

ALS data of the Kiihtelysvaara inventory area was collected on June 09, 2009 from 600 to 700 m above ground level. For the data collection, an ATM Gemini sensor (Optech, Canada) was used, and the field of view and swath width were 26° and 320 m, respectively. The sides overlap between the strips was 55 %. The average point density of the ALS data was 11.9 points m^{-2} (Packalén et al., 2013). The last echos of the data were interpolated into a digital terrain model (DTM) as they were considered as ground echoes (Axelsson, 2000) and the spatial resolution of the DTM was 0.5 m. The DTM was subtracted from the ALS echo heights to get the ALS returns above ground level. Echo heights lower than 0.1 m were also eliminated to avoid the terrain effect on the ALS metric computation because they were considered to be reflected from the ground surface. ALS returns of all concentric circular plots were clipped based on their coordinates (X_{sim}, Y_{sim}) and metrics were computed using FUSION/LDV software of the USDA Forest Service (McGaughey, 2021). ALS metrics are statistics that represent various forest characteristics such as L-skewness, L-coefficient of variation, Canopy relief ratio and Kurtosis of ALS height distributions which are related to the tree dominance, tree size inequality, vertical forest structure and distinguishing between young and mature forests, respectively (Table 1). These ALS metrics are used as auxiliary variables in the ALS-assisted estimation of various forest variables (Næsset, 2002; Maltamo et al., 2006).

For each concentric circular plot, we combined ALS metrics and their corresponding *BALM* values for all simulations carried out at all actual field plots. Then, we calculated the Pearson correlation coefficient (r) between *BALM* values and each ALS metric for increasing concentric circular plot size s (and the number of trees (sample size) n within). Since we were only interested that how ALS metrics explain the variability in *BALM* estimation regardless of whether the relationship is direct or indirect, we considered the absolute value of the correlation coefficient $|r|$.

2.5. Criteria for optimal plot size and sample size selection

The ALS-assisted estimation of any forest attribute in a plot and the sample size (number of trees n) within are essentially related to one another. Therefore, the relationship between predictors and response variables is affected by the sample size. Sample size refers either to the number of trees used to calculate the *BALM* or numbers of ALS returns (spatial resolution/point density) to compute the ALS metrics. Similarly, the sample size within a plot is also related to the actual densities of the stand (stand density (N; trees ha^{-1}) or ALS points density (d; points m^{-2})). Thus, the sample size or number of trees (n) within the concentric circular plot size s is linked with the stand density (N) of the original field plot by,

$$n = N\pi s^2 \tag{5}$$

A similar relationship also exists between the number of ALS returns

Table 1
Description of various ALS metrics and their representative forest characteristics.

Symbol/Description	proxy forest characteristics	Reference
L.skew/L-skewness	tree competition/ dominance	(Valbuena et al., 2017; Adnan et al., 2021)
L.cv/L-coefficient of variation	Tree size inequality	(Valbuena et al., 2017; Adnan et al., 2021)
IQ, Interquartile range	spread	(Hawryło et al., 2017)
AAD/Average absolute deviation	open vs closed canopy	(Adnan et al., 2021)
CRR/Canopy relief ratio	vertical forest structure	(Adnan et al., 2017)
Kur/Kurtosis	distinguishing young and mature forest	(Jones et al., 2012)

(p) within the same concentric circular plot size s and the ALS point density of the actual field plot (d) (Eq. (6)). This relationship also assures that the methodology can be replicated in any range of ALS point densities.

$$p = d\pi s^2 \tag{6}$$

Now, it is uncertain here whether the optimization should be based on plot size s (spatial resolution of ALS) or sample size n (point density p in case of ALS) or the relationship between *BALM* and ALS metrics is affected by plot size s or the number of trees n (or ALS returns p) within the plot size s because they both are related to one another. These relationships assure that the methodology adopted here can be applied to any range of stand densities N or point densities d and it is valid for both sparse and dense stand densities or ALS point densities. Now, to evaluate the effect of plot size and sample size (stand density) on the relationship between *BALM* and ALS metrics, the following two criteria were sequentially applied and repeated for the selection of both optimal plot size (s^*) and sample size (n^*).

Criterion i was focused on the stabilization of *BALM* values calculated from the field information itself. This criterion was achieved by observing the $\overline{BALM}_{diff}$ for an increasing plot size s or sample size n. The maximum value at which the estimation of *BALM* was considered as stable and representative of the total population was $\overline{BALM}_{diff} = 0.1$ relative to the mean *BALM*. This brings a different threshold for each forest area, which is good because the optimal is dependent on the *BALM* value itself. Any plot size s or sample size n which meets this criterion in all 79 actual field plots would be the minimum criterion for a stable *BALM* estimation.

Criterion ii was implemented to maximise the relationship between *BALM* and ALS metrics. This was achieved by combining all pairs of *BALM* values and their corresponding ALS metrics in each concentric circular plot from all 79 actual field plots. Those showing the maximum $|r|$ were selected as optimal plot size s^* or sample size n^*. There were more than 100 ALS metrics, we only selected the highly correlated metrics. These two criteria are summarised in the following Eqs. (7) and (8). All the above analyses were performed in R statistical software (R Core Team, 2021).

$$s^* = \overline{BALM}_{diff} < 0.1 \bullet \overline{BALM} | \max(|r|) \tag{7}$$

$$n^* = \overline{BALM}_{diff} < 0.1 \bullet \overline{BALM} | \max(|r|) \tag{8}$$

2.6. Evaluating the effects of ALS point density

To evaluate the effects of ALS point density on the relationship between *BALM* values and ALS metrics, we chose the optimal plot size s^* decided in the previous step. First, we reduced the original point density of 11.9 points m^{-2} to 0.50, 0.75, 1, 3, 5, 7.5, and 10 points m^{-2}. For this purpose, we identified a correct thinning factor for each desired point density d (Adnan et al., 2017) and applied procedures available in the Lastools software (RapidLasso GmbH Inc.; Isenburg, 2016). From each reduced point density d, new ALS metrics were computed in all k simulations and each concentric circular plot. The new ALS metrics were correlated with the *BALM* values as it was carried out for s and n and the effects of varying ALS point densities on the relationship were evaluated.

3. Results

3.1. Deciding the minimum number of simulations based on sensitivity analysis

The results of the sensitivity analysis to select the minimum number of simulations are shown in Fig. 4. In any number of simulations (10, 50, 100, 500, 700 and 1000), the *BALM* values were unstable in the smaller concentric circular plots, and as the size of the plot increased, the *BALM* value stabilised and approached to the value of the actual field plot ($\overline{BALM}_{ref}$) (Fig. 4a). However, the difference between different numbers of simulations was more visible in Fig. 4b which shows how the standard error of mean (SEM) decreased as the number of simulations increased. In the initial 10 simulations, the SEM highly fluctuated in all concentric circular plot sizes 1–15 m and as the number of simulations increased, the *BALM* value approached to stabilise. From 500 to 1000 number of simulations, the variation in SEM was very minor, particularly in the smaller concentric circular plots, but virtually no variation was observed in the higher concentric circular plots. Thus, we opted to use minimum $k = 500$ simulations in each actual field plot (79 in total) that would produce a stable and robust *BALM* estimation.

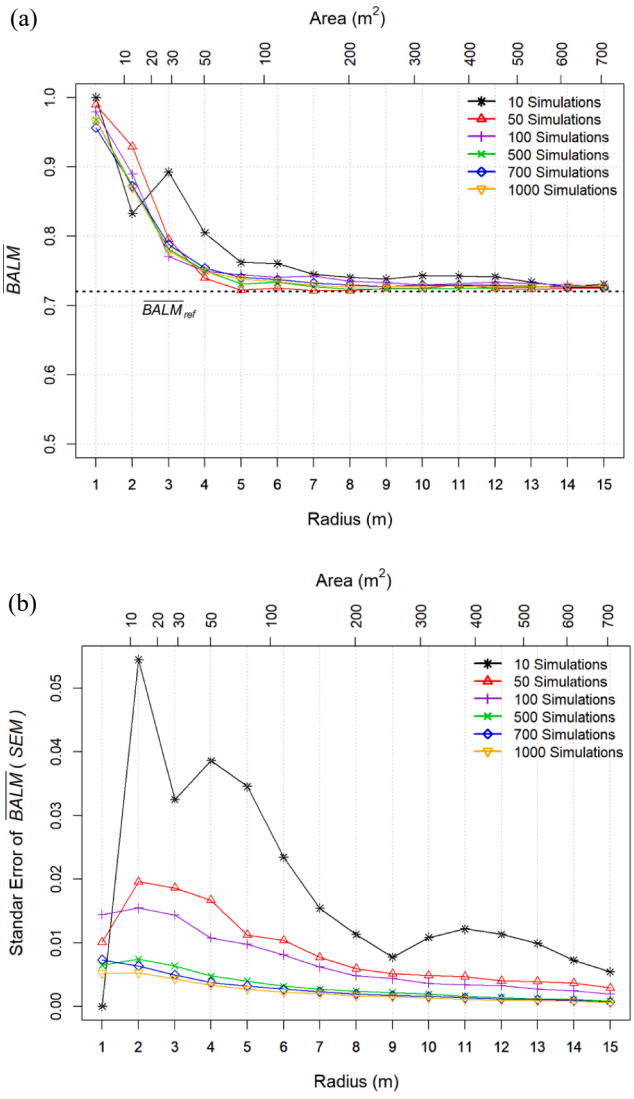

Fig. 4. Selection of minimum number of simulations based on sensitivity analysis. Evolution of (a) $\overline{BALM}$ and the (b) the standard error of mean for increasing concentric circular plots (1–15 m radii) and the number of simulations (10–1000).

3.2. Optimal plot size and sample size selection

Figs. 5 and 6 show the results of the two criteria adopted to select the optimal plot size and sample size for a reliable *BALM* estimation. In Fig. 5a, the $\overline{BALM}_{diff}$ values of all 79 actual field plots are given for increasing concentric circular plots 1–15 m radii and their maximum (solid horizontal line at 0.095) and minimum (dashed horizontal lines at

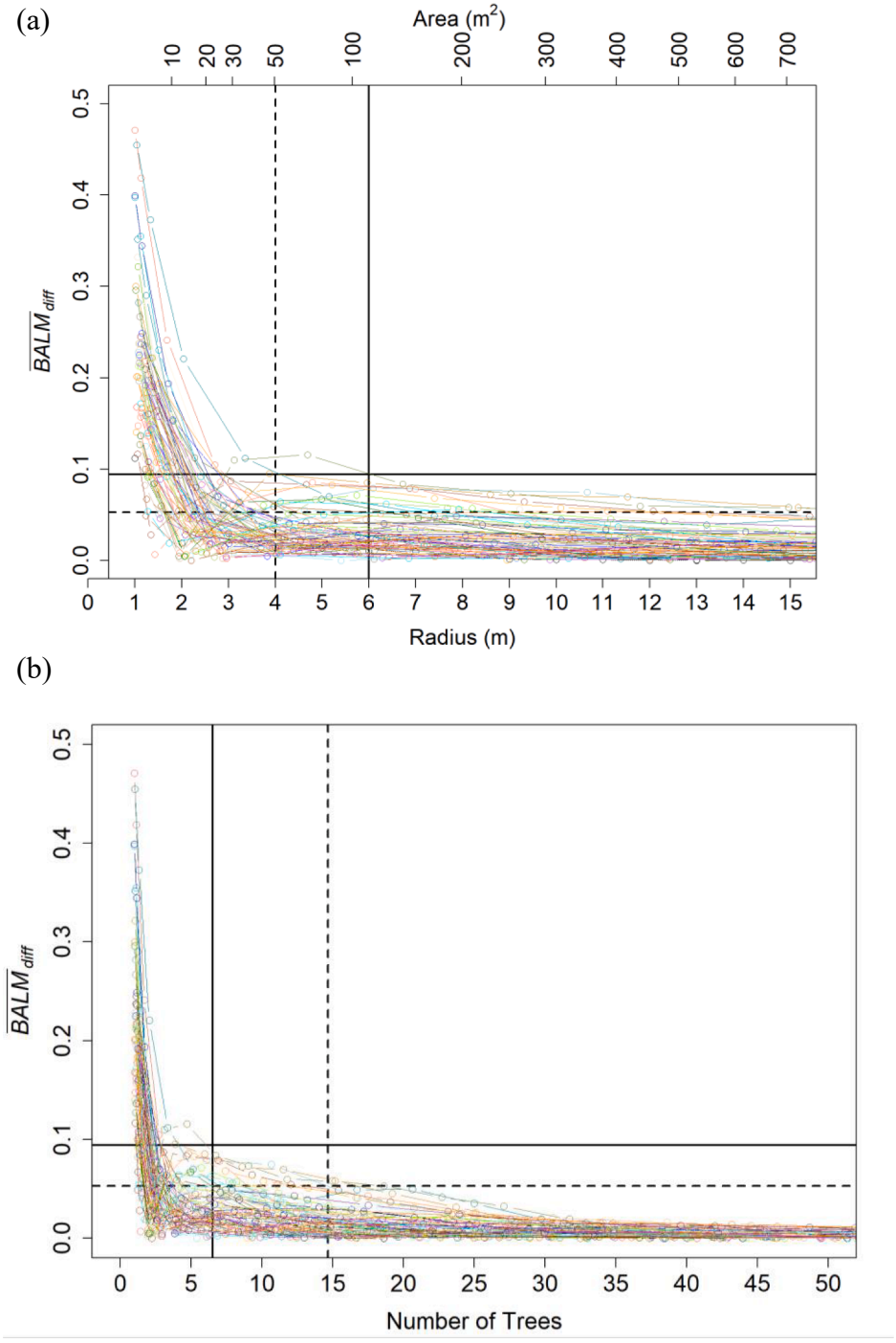

Fig. 5. Results of the *Criterion i* which show the $\overline{BALM}_{diff}$ in all 79 actual field plots (coloured lines) for increasing (a) concentric circular plots (1–15 m radii) and (b) the number of trees (sample size). The horizontal lines (solid and dashed) show the maximum and minimum $\overline{BALM}_{diff}$ limit imposed to obtain stable estimation while the vertical solid lines denote the minimum plot sizes and sample sizes for stable *BALM* estimation.

0.052) threshold limits. In smaller concentric circular plots, the *BALM* values were highly unstable and not representative of the actual field plots ($\overline{BALM}_{ref}$), but as the size of the concentric circular plot increased, the *BALM* values stabilised. At the plot size $s \geq 6$ m, all $\overline{BALM}_{diff}$ values were less than the maximum threshold limit (0.095), while at plot size $s \geq 4$ m fewer plots were within the minimum threshold limit (0.052). We estimate that based on the threshold limits, a plot size $s \geq 6$ m (approximately 113 m^2) could be the minimum plot size to obtain a stable *BALM* estimation because any increase beyond this would not considerably improve the results.

Table 2 also affirms these results because the proportion of actual field plots to reach stabilisation increased as the size of the concentric circular plot increased. For example, in the concentric circular plot size $s = 1$ m radius, only 15.2 % of actual field plots were within the required limit but at the concentric circular plot size $s = 6$ m radius, all actual field plots (100 %) were below the required limit of $\overline{BALM}_{diff} < 0.1 \bullet \overline{BALM}$. Thus, concentric circular plot size $s = 6$ m radius could be the minimum plot size for a stable *BALM* estimation. With regards to the *Criterion ii* which shows the absolute correlation $|r|$ between the *BALM* estimation and various ALS metrics (*Kur*, *IQ*, *L.cv*, *L.*

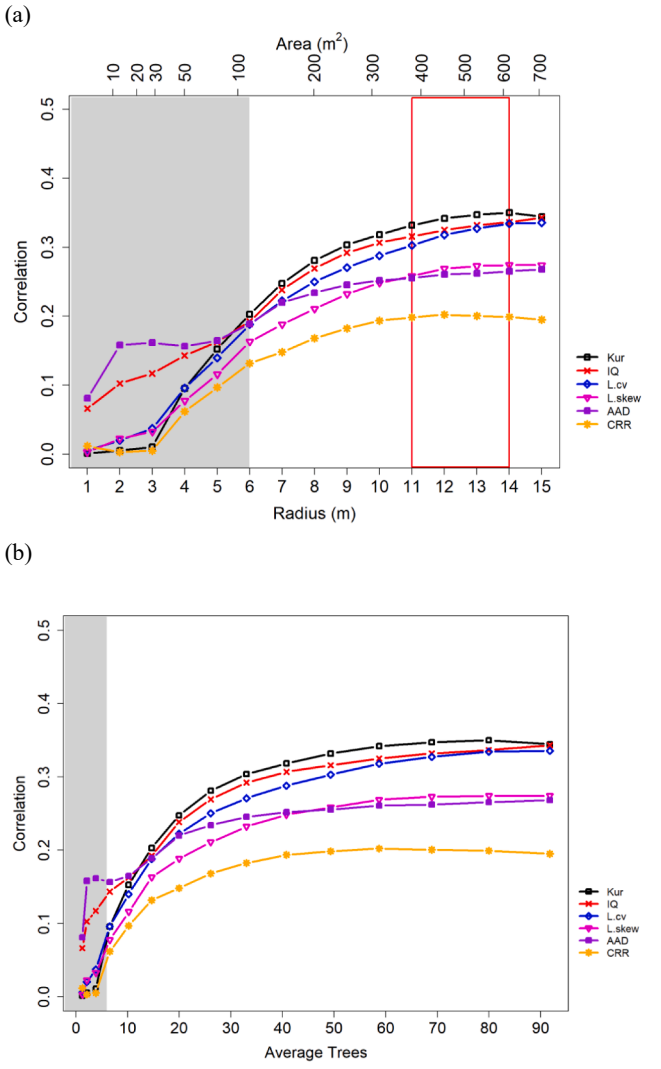

Fig. 6. Results showing the absolute correlation $|r|$ between *BALM* values and various ALS metrics (explanation given in Table 1) for increasing (a) concentric circular plots $s = 1-15$ m radii and (b) sample sizes ($n = 1-90$ average number of trees) (*Criterion ii*). The red rectangle shows the optimal plot size $s^* = 11-14$ m radii for reliable *BALM* estimation. The corresponding area is also given on the upper axis.

skew, *AAD*, and *CRR*) (Table 1, Fig. 6a), similar inconsistencies in the correlation were found in the smaller concentric circular plots due to the unstable estimation of *BALM* (Fig. 5a). This also showed the importance of implementing *Criterion i* as a prior step in which the smaller concentric circular plots were already dismissed. This dismissed area is shaded in grey colour in Fig. 6a.

Once the *BALM* estimation reached stabilisation at concentric circular plot size $s = 6$ m radius, the correlation between *BALM* values and ALS metrics followed a particular trend. The trend was more visible in the highly correlated ALS metrics such as *Kur*, *L.cv*, and *L.skew*, and priority was given to these ALS metrics for the plot size optimization. The trend followed a convex curve, from which it was possible to select a maximum correlation and establish the optimal plot size for a reliable *BALM* estimation. In the trend, all ALS metrics showed a high correlation from concentric circular plot size 11 to 14 m radii which could be the optimal plot sizes (s^*) for reliable ALS-assisted *BALM* estimation. From concentric circular plot size $s > 14$ m radius, the ALS metrics showed a decreasing trend, for example, in *Kur*, *L.cv*, *L.skew*, and *CRR*. In summary, the minimum plot size for reliable and robust *BALM* estimation

Table 2
The proportion of actual field plots and the minimum number of trees required in each concentric circular plot to reach stabilization (*Criterion i*).

The radius of the concentric circular plot (m)	The proportion of actual field plots (%) reaching stabilisation ($\overline{BALM}_{diff} < 0.1 \bullet \overline{BALM}$)	Minimum number of trees required to reach stabilisation	Average number of trees required to reach stabilisation
1	15.2	1	1
2	63.3	1	2
3	93.7	2	4
4	96.2	3	6
5	98.7	4	10
6	100	6	15
7	100	7	20
8	100	9	26
9	100	12	33
10	100	15	41
11	100	18	49
12	100	21	59
13	100	25	69
14	100	29	80
15	100	33	92

should be at least 113 m^2 (6 m radius) while the optimal plot size s^* could be approximately 380–615 m^2 area (11–14 m radii).

The results of *Criterion i* and *ii* that how the sample size (stand density) affects the relationship between the *BALM* estimation and ALS metrics are shown in Fig. 5b and 6b. Fig. 5b shows the evolution of $\overline{BALM}_{diff}$ against the sample size (number of trees n within the concentric circular plots) in all 79 actual field plots and their maximum (solid horizontal line at 0.095) and minimum (dashed horizontal lines at 0.052) threshold limits. We obtained similar results as Fig. 5a because the plot size s relates to the number of trees n (sample size) according to Eq. (5). The $\overline{BALM}_{diff}$ highly fluctuated in smaller sample sizes because they were not representative of the stand density N of the actual field plot and thus the estimation of *BALM* was unstable. For example, in concentric circular plot sizes $s = 1-4$ m radii, at least 1–3 trees were required to reach stabilization ($\overline{BALM}_{diff} < 0.1 \bullet \overline{BALM}$) but in 84.8 %, 36.7 %, 6.3 % and 3.6 % of the actual field plots, respectively, the minimum number of trees n in the 1–4 m concentric circular plots was less (Table 2). At the sample size $n \geq 15$ trees, some plots were above the required limit, but at the sample size $n \geq 6$ trees, the $\overline{BALM}_{diff}$ in all 79 actual field plots were below the required $\overline{BALM}_{diff} < 0.1 \bullet \overline{BALM}$ limit and this could be the minimum number of trees (sample size) required for a stable *BALM* estimation in our study (Fig. 5b). However, the sample size also depends on the overall tree density of a stand. Areas with sparse stand density will require a smaller sample size and vice versa as shown in Fig. 7.

To optimize the number of trees (sample size), the *BALM* values were correlated with the same ALS metrics, but this time with the increasing number of trees n instead of the concentric circular plot size s (*Criterion ii*). The absolute correlation $|r|$ obtained in Fig. 6b was similar to Fig. 6a as they also relate to each other according to Eq. (5). Instability in the correlation was found for the smaller sample sizes (number of trees n) but as the sample size increased, the correlation followed a similar convex curve. Here, the optimal sample size n^* could also be reliably determined from the highest correlation. In this case, the maximum absolute correlation was found between 50 and 80 trees which could be the optimal sample size n^* for the ALS-assisted *BALM* estimation (Fig. 6b).

3.3. ALS point density effect on the relationship between BALM and ALS metrics

In the previous results, we obtained that the optimal plot size s^* for

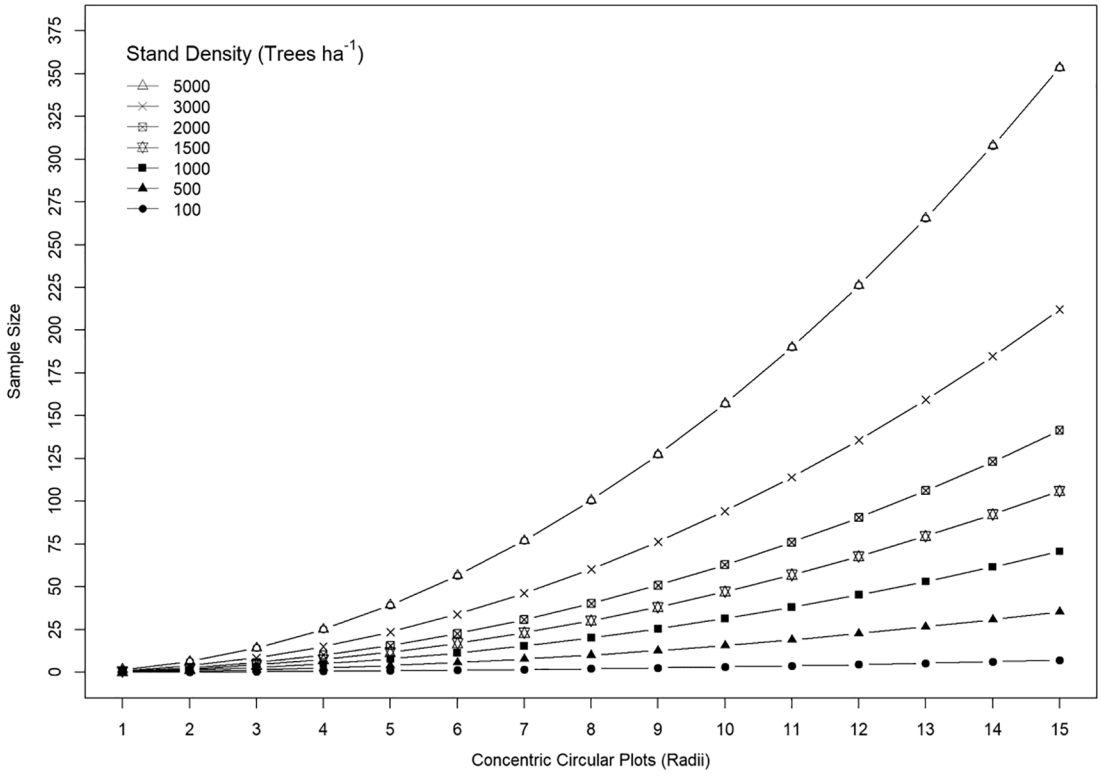

Fig. 7. Determining the sample size under different stand densities in concentric circular plots 1–15 m using Eq. (5).

ALS-assisted *BALM* estimation ranges from 11 to 14 m radii. Therefore, to evaluate the point density effect and facilitate direct comparison, we chose an optimal plot size $s^* = 14$ m radius and employed the same ALS metrics as in the previous steps (*Kur*, *IQ*, *L.cv*, *L.skew*, *AAD*, and *CRR*). The results are presented in Fig. 8 which shows the absolute correlation $|r|$ between *BALM* values and ALS metrics for an increasing number of point density *d*. Some irregularities have been found in the relationship if the point density is less than 5 points m^{-2} but for higher ALS point densities, no major effects have been observed. Therefore, any ALS point density $d \geq 5$ points m^{-2} would be suitable for reliable *BALM* estimation using ALS. Thus, the relationship between *BALM* estimation and ALS metrics is mostly independent of the sample size (stand density) or ALS point density but depends on the plot size employed.

4. Discussion

Basal area larger than mean (*BALM*) is an important indicator that can be used to separate different forest structural types (FSTs) and measure the cohort balance in forests. However, this structural indicator was largely ignored by the scientific community until Gove (2004)

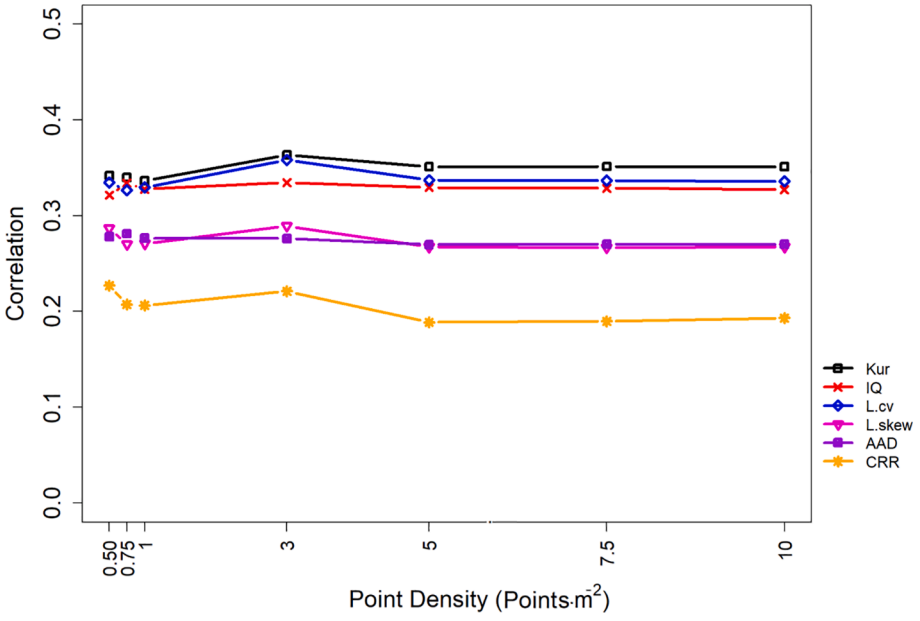

Fig. 8. The effect of airborne laser scanning point density on the relationship between *BALM* and ALS metrics. The explanation of the ALS metrics is given in Table 1.

identified and described its importance in the prescription of silvicultural activities. Valbuena et al. (2013) later hypothesized that *BALM* together with the Gini coefficient of tree size inequality are the two important variables for structural characterisation. Based on this assumption, Adnan et al. (2019) applied different forest attributes including *BALM* and conducted a bioregional forest structural heterogeneity assessment. Their study confirmed the assumption and found that the *BALM* together with the Gini coefficient of tree size inequality were superior to the stand density and quadratic mean diameter (D_{QMD}) in the structural classification of forests. Lower, medium and high *BALM* values explicitly separated single-layered, multi-layered, and reversed-J types of forest structures, respectively. However, they also noticed that different plot sizes in their sites could affect the estimated values of the forest attributes including *BALM*. The effect of plot size on the stand density, quadratic mean diameter (D_{QMD}) and Gini coefficient of tree size inequality is well documented (Gray, 2003; Ruiz et al., 2014; Adnan et al., 2017; Häbel et al., 2019) but the plot size effect on the *BALM* estimation is still unknown. This observation motivated the current study to evaluate the plot size, sample size (number of trees), and ALS point density effects on the relationship between *BALM* estimates and airborne laser scanning (ALS) metrics.

A key question at this juncture is: why does it matter to choose an optimal plot size? For any forest attribute, optimal plot size is important because inoptimal plot sizes may produce unreliable results that could lead to imprecise decisions in forest management (Eid, 2000). Similarly, both smaller and larger plot sizes have their own consequences. For example, if the plot size is small, it affects the stem diameter distribution (Maltamo et al., 2019). But on the other hand, if the plot size is large, it increases the field measurement, time, and cost (Chytrý and Otýpková, 2003). The selection of optimal plot size is also not straightforward, and it varies from one forest type to another (Häbel et al., 2019). It depends on various factors such as the purpose of inventory, variable of interest, time, field measurement, and cost (Henttonen and Kangas, 2015).

The variance in the estimated values of a forest attribute decreases with the increasing size of a plot (Kukunda et al., 2019) because, in the smaller plot sizes, the lower number of trees n (sample size) underrepresent the tree density N of the population. This tendency can be seen in Fig. 5 where the $\overline{BALM}_{diff}$ values in a majority of the actual field plots were highly unstable in the smaller concentric circular plots (1–5 m radii) and sample sizes ($n < 6$ trees) due to the high variance, but as the plot size and sample size increased, variance decreased and the estimated *BALM* value approached the reference value ($\overline{BALM}_{ref}$) of the actual field plot (Fig. 4). Similar results have been obtained by Johnson and Hixon (1952), Barbeito et al. (2009), Matos (2014), and Adnan et al. (2017) and it is now well established that the accuracy of the estimated forest attributes increases and bias decreases when the size of a plot increases. At the concentric circular plot size $s = 6$ m radius and sample size $n = 6$ trees, $\overline{BALM}_{diff}$ in all 79 actual field plots fell below the required $\overline{BALM}_{diff} < 0.1 \bullet \overline{BALM}$ limit and followed *Criterion i* that is the stabilisation of the *BALM* values. Thus, the area/spatial resolution covering approximately 113 m^2 (6 m radius) could be the minimum plot size for a stable *BALM* estimation (Fig. 5). The minimum plot size could also vary according to the density of a stand, for example, sparse tree density stands would require a larger plot size and dense tree stands would comparatively require a smaller plot size (Lombardi et al., 2015). This variability in stand density could be adjusted according to Eq. (5) of this study which brings generality to our methods and the study presented here could be replicated in any forest stand density (Fig. 7).

We were interested to maximise the relationship between *BALM* estimates and ALS metrics and obtain the most reliable results. Fig. 6 shows the absolute correlation $|r|$ between *BALM* values and various ALS metrics for an increasing plot size s (Fig. 6a) and sample size (number of trees) n (Fig. 6b). Among numerous ALS metrics, we only chose the most correlated ones such as *Kur*, *IQ*, *L.cv*, *L.skew*, *AAD*, and *CRR* (explanation given in Table 1). These chosen ALS metrics represent various aspects of forest structures, for example, *L.skew* describes the tree dominance or competitive condition which is very relevant to the *BALM* (Adnan et al., 2019). A negative *L.skew* is obtained when laser pulses hit closed canopies represented by high *BALM* values because only a small portion of ALS pulses would penetrate, and a major portion would backscatter. On the other hand, the *L.skew* would be positive, if the canopy is open (lower *BALM* values) because a major portion of the ALS pulses would penetrate in this case (Valbuena et al., 2017). Therefore, either *BALM* calculated from field data or *L.skew* obtained directly from ALS data could be useful to analyse open and closed canopy forests or describe light availability in forest stands. Similarly, Jones et al. (2012) found that young and mature forests could only be discriminated by *Kur* which is again relevant to the *BALM* as it accumulates the proportion of basal areas of all trees with $dbh \geq D_{QMD}$ (Eq. (1)). Now, looking at Fig. 6(a, b), the absolute correlation $|r|$ between *BALM* and the chosen ALS metrics followed a convex curve. It can also be seen that the correlation at the smaller plot sizes and the sample sizes was unstable. This is because the lower sample size was not representative of the overall tree density of the actual field plots, and it was important to impose the first criterion (*Criterion i*). This area is shaded in grey colour in Fig. 6, which means that the lower plot sizes ($s = 1 - 5$ m radii) and sample sizes ($n < 6$ trees) are already eliminated and not suitable for a reliable *BALM* estimation. As the plot size increased, the sample size became more representative of the tree density of the actual field plots and thus the maximum absolute correlation was found in concentric circular plot sizes 11–14 m radii (380–615 m^2 area) which could be the optimal plot sizes (s^*) for the ALS-assisted *BALM* estimation. From concentric circular plot size $s = 14$ m radius onwards, the correlation showed a decreasing trend, for example, in *Kur*, *L.skew*, and *CRR* (Fig. 6a). Similarly, in sample size optimization, the maximum absolute correlation was found between sample size 50–80 trees which could be the optimal sample size (n^*) for a reliable *BALM* estimation using the ALS data.

The optimal plot sizes ($s^* = 11 - 14$ m radii or 380–615 m^2 area) obtained in our study coincide with the recommended plot sizes obtained in other studies such as 13–15 m radii for describing heterogeneity in old stand growth (Lombardi et al., 2015), 9–12 m radii for ALS assisted Gini coefficient estimation (Adnan et al., 2017; Adnan, 2020) and 200–400 m^2 for stand-level stem diameter distribution in Finland (Maltamo et al., 2019). However, there are still differences with the routines of the current ALS forest inventory in Finland. For example, larger plots are employed in the young stands and thus the attributes measurement takes a longer time, and the total number of field plots is less as compared to the other stand types.

ALS surveys usually cover large geographical areas and due to the rough topography and different forest conditions, the point density specified on the ground varies from one place to another. And when the adjacent strips overlap, the variation in point densities is even more (Gobakken and Næsset, 2008). This study was conducted in a flat area where the original point density (average) was 11.9 points m^{-2}. When the ALS point density effect on the *BALM* estimation was evaluated, no major effects on the relationship between *BALM* values and ALS metrics were found unless the point density $d < 5$ points m^{-2} (Fig. 8). Similar results have been obtained in various other studies that the ALS point density has very marginal effects on the estimated forest attributes, for example, volume (Maltamo et al., 2006; Ruiz et al., 2014), biomass (Singh et al., 2015), mean tree height and stand basal area (Gobakken and Næsset, 2008) and the Gini coefficient of tree size inequality (Adnan et al., 2017). However, it must be noted that in this study, the same digital terrain model (DTM) based on the original point density was used following Maltamo et al. (2006). According to Ruiz et al. (2014), DTM based on sparser point density may incur some uncertainties, but Magnusson (2006) found a stable and unbiased DTM up to the 0.01 points m^{-2} thinning level. So, we proclaim that the thinned point densities have more prominent effects on the forest attributes than the terrain. The National Land Survey of Finland (NLS) is currently acquiring the

nationwide ALS data (second round) with a point density of approximately 5 points m^{-2} and based on our results, this point density of the current national ALS survey is suitable for the forest structural assessment. It would also provide new possibilities to monitor the forest resources of the country with much better accuracy.

5. Conclusions

This study was conducted in a typical boreal forest in Finland to analyze the relationship between *BALM* estimates and ALS metrics and how the varying plot size, sample size (number of trees), and ALS point density affect this relationship. As the plot size determines both the stand and scan densities, their effects are interdependent. For a reliable ALS assisted *BALM* estimation, two criteria were implemented in this study that is the stabilization of the *BALM* estimates (*Criterion i*) and the maximization of the absolute correlation between *BALM* estimates and ALS metrics (*Criterion ii*). We found that the *BALM* estimates and their absolute correlation with ALS metrics were highly unstable at the smaller concentric circular plots (1–5 m radii) and sample sizes (>6 trees) because the smaller concentric circular plots contained smaller sample sizes which underrepresented the tree density of the actual field plots. As the plot size increased, the sample size became more representative of the actual field plot. At the concentric circular plot size 6 m radius and sample size 6 trees, the *BALM* estimates stabilized and followed the first criterion which could be the minimum plot size and sample size for stable *BALM* estimation. Regarding *Criterion ii*, the maximum correlation was found between concentric circular plot size 11–14 m radii (380–615 m^2 area) and sample size 50–80 trees which could be the optimal plot size and sample size for ALS assisted *BALM* estimation. From the analysis of the point density effect, we concluded that at least 5 points m^{-2} are needed for reliable *BALM* estimation. Any point density lesser than this would be unsuitable. The point density of the current nationwide ALS survey is also 5 points m^{-2} and our results support that it is suitable for the forest structural assessment. Results presented in this study could help the forestry practitioner to develop more reliable stocking guides which are the decision-making process about silvicultural activities in forest stands and bring about better estimation mapping of ecological diversity at large scales using ALS data.

CRediT authorship contribution statement

Syed Adnan: Conceptualization, Funding acquisition, Data curation, Methodology, Formal analysis, Software, Writing – original draft. **Rubén Valbuena:** Supervision, Writing – review & editing. **Tuomo Kauranne:** Writing – review & editing. **Ranjith Gopalakrishnan:** Writing – review & editing. **Matti Maltamo:** Resources, Supervision, Funding acquisition, Writing – review & editing.

Declaration of Competing Interest

The authors declare that they have no known competing financial interests or personal relationships that could have appeared to influence the work reported in this paper.

Data availability

Data will be made available on request.

Acknowledgements

The author Syed Adnan would like to thank the Finnish Society of Forest Science (Suomen Metsätieteellinen Seura, grants decision 2021) and PostDocs in Companies (PoDoCo) program of the Foundation for Economic Education (Liikesivistysrahasto, grant number: 210018) for financing and supporting this research. This work was also supported by the Finnish Flagship Programme of the Academy of Finland for the Forest-Human-Machine Interplay - Building Resilience, Redefining Value Networks and Enabling Meaningful Experiences (UNITE) - project (decision number 337127), led by Prof. Jyrki Kangas at the School of Forest Sciences, University of Eastern Finland. We would like to thank the reviewers for their constructive comments and suggestions.

References

Adnan, S., Maltamo, M., Coomes, D.A., Valbuena, R., 2017. Effects of plot size, stand density, and scan density on the relationship between airborne laser scanning metrics and the Gini coefficient of tree size inequality. Can. J. For. Res. 47 (12), 1590–1602.

Adnan, S., Maltamo, M., Coomes, D.A., García-Abril, A., Malhi, Y., Manzanera, J.A., Butt, N., Morecroft, M., Valbuena, R., 2019. A simple approach to forest structure classification using airborne laser scanning that can be adopted across bioregions. For. Ecol. Manage. 433, 111–121.

Adnan, S., Maltamo, M., Mehtätalo, L., Ammaturo, R.N.L., Packalen, P., Valbuena, R., 2021. Determining maximum entropy in 3D remote sensing height distributions and using it to improve aboveground biomass modelling via stratification. Remote Sens. Environ. 260, 112464.

Adnan, S., 2020. Improvements in forest structural type assessment using airborne laser scanning. Dissert. Forestales 306, 1–60. https://doi.org/10.14214/df.306.

Almeida, D.R.A., Stark, S.C., Chazdon, R., Nelson, B.W., Cesar, R.G., Meli, P., Gorgens, E. B., Duarte, M.M., Valbuena, R., Moreno, V.S., Mendes, A.F., Amazonas, N., Gonçalves, N.B., Silva, C.A., Schietti, J., Brancalion, P.H.S., 2019. The effectiveness of lidar remote sensing for monitoring forest cover attributes and landscape restoration. For. Ecol. Manage. 438, 34–43.

Axelsson, P., 2000. DEM generation from laser scanner data using adaptive TIN models. Int. Arch. Photogramm. Remote Sens. 33 (4), 110–117.

Barbeito, I., Cañellas, I., Montes, F., 2009. Evaluating the 43tilizat of vertical structure indices in Scots pine forests. Ann. Forest Sci. 66, 710.

Chytrý, M., Otýpková, Z., 2003. Plot sizes used for phytosociological sampling of European vegetation. J. Veg. Sci. 14 (4), 563–570.

Coomes, D.A., Allen, R.B., 2007. Mortality and tree-size distributions in natural mixed-age forests. J. Ecol. 95 (1), 27–40.

Coomes, D.A., Šafka, D., Shepherd, J., Dalponte, M., Holdaway, R., 2018. Airborne laser scanning of natural forests in New Zealand reveals the influences of wind on forest carbon. For. Ecosyst. 5 (1), 1–14.

Davenport, I.J., Holden, N., Gurney, R.J., 2004. Characterizing errors in airborne laser altimetry data to extract soil roughness. IEEE Trans. Geosci. Remote Sens. 42 (10), 2130–2141.

Eid, T., 2000. Use of uncertain inventory data in forestry scenario models and consequential incorrect harvest decisions. Silva Fennica 34 (2), 89–100.

Gaveau, D.L., Hill, R.A., 2003. Quantifying canopy height underestimation by laser pulse penetration in small-footprint airborne laser scanning data. Canad. J. Remote Sens. 29 (5), 650–657.

Gobakken, T., Næsset, E., 2008. Assessing effects of laser point density, ground sampling intensity, and field sample plot size on biophysical stand properties derived from airborne laser scanner data. Can. J. For. Res. 38 (5), 1095–1109.

Goodwin, N.R., Coops, N.C., Culvenor, D.S., 2006. Assessment of forest structure with airborne LiDAR and the effects of platform altitude. Remote Sens. Environ. 103 (2), 140–152.

Gotway, C.A., Young, L.J., 2002. Combining incompatible spatial data. J. Am. Stat. Assoc. 97 (458), 632–648.

Gove, J.H., 2004. Structural stocking guides: a new look at an old friend. Can. J. For. Res. 34, 1044–1056.

Gove, J.H., Patil, G.P., 1998. Modeling the basal area-size distribution of forest stands: a compatible approach. For. Sci. 44 (2), 285–297.

Gray, A., 2003. Monitoring stand structure in mature coastal Douglas-fir forests: effect of plot size. For. Ecol. Manage. 175 (1–3), 1–16.

Häbel, H., Kuronen, M., Henttonen, H.M., Kangas, A., Myllymäki, M., 2019. The effect of spatial structure of forests on the precision and costs of plot-level forest resource estimation. For. Ecosyst. 6 (1), 1–11.

Hauglin, M., Rahlf, J., Schumacher, J., Astrup, R., Breidenbach, J., 2021. Large scale mapping of forest attributes using heterogeneous sets of airborne laser scanning and National Forest Inventory data. For. Ecosyst. 8 (1), 1–15.

Hawryło, P., Tompalski, P., Wężyk, P., 2017. Area-based estimation of growing stock volume in Scots pine stands using ALS and airborne image-based point clouds. For.: Int. J. For. Res. 90 (5), 686–696.

Henttonen, H.M., Kangas, A., 2015. Optimal plot design in a multipurpose forest inventory. For. Ecosyst. 2 (1), 31.

Hollaus, M., Dorigo, W., Wagner, W., Schadauer, K., Höfle, B., Maier, B., 2009. Operational wide-area stem volume estimation based on airborne laser scanning and national forest inventory data. Int. J. Remote Sens. 30 (19), 5159–5175.

Holmgren, J., Nilsson, M., Olsson, H., 2003. Simulating the effects of lidar scanning angle for estimation of mean tree height and canopy closure. Canad. J. Remote Sens. 29 (5), 623–632.

Isenburg, M., 2016. LAStools — efficient tools for LiDAR processing (Version 160921, academic) [online]. Available from http://rapidlasso.com/LAStools.

Johnson, F.A., Hixon, H.J., 1952. The most efficient size and shape of plot to use for cruising in old-growth Douglas-fir timber. J. For. 50 (1), 17–20.

Jones, T.G., Coops, N.C., Sharma, T., 2012. Assessing the utility of LiDAR to differentiate among vegetation structural classes. Remote Sens. Lett. 3 (3), 231–238.
Kaartinen, H., Hyyppä, J., Yu, X., Vastaranta, M., Hyyppä, H., Kukko, A., Holopainen, M., Heipke, C., Hirschmugl, M., Morsdorf, F., Næsset, E., Pitkänen, J., Popescu, S., Solberg, S., Wolf, B.M., Wu, J.-C., 2012. An international comparison of individual tree detection and extraction using airborne laser scanning. Remote Sens. 4 (4), 950–974.
Kukunda, C.B., Beckschäfer, P., Magdon, P., Schall, P., Wirth, C., Kleinn, C., 2019. Scale-guided mapping of forest stand structural heterogeneity from airborne LiDAR. Ecol. Ind. 102, 410–425.
Lessard, V.C., McRoberts, R.E., Holdaway, M.R., 2001. Diameter growth models using Minnesota Forest Inventory and Analysis data. For. Sci. 47 (3), 301–310.
Lombardi, F., Marchetti, M., Corona, P., Merlini, P., Chirici, G., Tognetti, R., Burrascano, S., Alivernini, A., Puletti, N., 2015. Quantifying the effect of sampling plot size on the estimation of structural indicators in old-growth forest stands. For. Ecol. Manage. 346, 89–97.
Magnusson, M., 2006. Evaluation of remote sensing techniques for estimation of forest variables at stand level, Vol. 2006, No. 2006, 85).
Maltamo, M., Eerikäinen, K., Pitkänen, J., Hyyppä, J., Vehmas, M., 2004. Estimation of timber volume and stem density based on scanning laser altimetry and expected tree size distribution functions. Remote Sens. Environ. 90 (3), 319–330.
Maltamo, M., Packalén, P., Yu, X., Eerikäinen, K., Hyyppä, J., Pitkänen, J., 2005. Identifying and quantifying structural characteristics of heterogeneous boreal forests using laser scanner data. For. Ecol. Manage. 216 (1–3), 41–50.
Maltamo, M., Eerikäinen, K., Packalén, P., Hyyppä, J., 2006. Estimation of stem volume using laser scanning-based canopy height metrics. Forestry 79 (2), 217–229.
Maltamo, M., Næsset, E., Vauhkonen, J., 2014. Forestry applications of airborne laser scanning. Concepts and case studies. Manag. For. Ecosys. 27, 2014.
Maltamo, M., Mehtätalo, L., Valbuena, R., Vauhkonen, J., Packalen, P., 2018. Airborne laser scanning for tree diameter distribution modelling: a comparison of different modelling alternatives in a tropical single-species plantation. For. Int. J. For. Res. 91 (1), 121–131.
Maltamo, M., Hauglin, K.M., Næsset, E., Gobakken, T., 2019. Estimating stand level stem diameter distribution utilizing accurately positioned tree-level harvester data and airborne laser scanning. Silva Fennica 53 (3), id 10075.
Maltamo, M., Kinnunen, H., Kangas, A., Korhonen, L., 2020. Predicting stand age in managed forests using National Forest Inventory field data and airborne laser scanning. For. Ecosyst. 7 (1), 1–11.
Matos, A., 2014. Effect of scale factor in estimation of Gini coefficient [online]. M.Sc. thesis, University of Eastern Finland. Available from http://urn.fi/urn:nbn:fi:uef-20140718 and www.oppi.uef.fi/opk/video/europeanforestry/a_matos_seminar.mp4 [accessed August 2021].
McGaughey, R.J., 2021. FUSION/LDV: software for LIDAR data analysis and visualization. Version 4.21. USDA Forest Service, Pacific Northwest Research Station. [accessed September 2021].
Melin, M., Packalén, P., Matala, J., Mehtätalo, L., Pusenius, J., 2013. Assessing and modeling moose (Alces alces) habitats with airborne laser scanning data. Int. J. Appl. Earth Obs. Geoinf. 23, 389–396.
Mononen, L., Auvinen, A.P., Packalén, P., Virkkala, R., Valbuena, R., Bohlin, I., Valkama, J., Vihervaara, P., 2018. Usability of citizen science observations together with airborne laser scanning data in determining the habitat preferences of forest birds. For. Ecol. Manage. 430, 498–508.
Naesset, E., 1997. Estimating timber volume of forest stands using airborne laser scanner data. Remote Sens. Environ. 61 (2), 246–253.
Næsset, E., 2002. Predicting forest stand characteristics with airborne scanning laser using a practical two-stage procedure and field data. Remote Sens. Environ. 80 (1), 88–99.
Næsset, E., Økland, T., 2002. Estimating tree height and tree crown properties using airborne scanning laser in a boreal nature reserve. Remote Sens. Environ. 79 (1), 105–115.
Oboite, F.O., Comeau, P.G., 2019. Competition and climate influence growth of black spruce in western boreal forests. For. Ecol. Manage. 443, 84–94.
Otypková, Z., Chytry, M., 2006. Effects of plot size on the ordination of vegetation samples. J. Veg. Sci. 17, 465–472. https://doi.org/10.1111/j.1654-1103.2006.tb02467.x.
Packalén, P., Maltamo, M., 2006. Predicting the plot volume by tree species using airborne laser scanning and aerial photographs. For. Sci. 52 (6), 611–622.
Packalén, P., Vauhkonen, J., Kallio, E., Peuhkurinen, J., Pitkänen, J., Pippuri, I., Strunk, J., Maltamo, M., 2013. Predicting the spatial pattern of trees by airborne laser scanning. Int. J. Remote Sens. 34 (14), 5154–5165.
Päivinen, R., 1987. Metsän inventoinnin suunnittelumalli. [A planning model for forest inventory, In Finnish]. 11th edn. University of Joensuu publications in Sciences, University of Joensuu, Joensuu.
Pedersen, R.Ø., Bollandsås, O.M., Gobakken, T., Næsset, E., 2012. Deriving individual tree competition indices from airborne laser scanning. For. Ecol. Manage. 280, 150–165.
Pippuri, I., Kallio, E., Maltamo, M., Peltola, H., Packalén, P., 2012. Exploring horizontal area-based metrics to discriminate the spatial pattern of trees and need for first thinning using airborne laser scanning. Forestry 85 (2), 305–314.
Pommerening, A., Stoyan, D., 2006. Edge-correction needs in estimating indices of spatial forest structure. Can. J. For. Res. 36 (7), 1723–1739.
R Core Team, 2021. R: a language and environment for statistical computing [online]. Available from, R Foundation for Statistical Computing, Vienna, Austria http://www.R-project.org.
Ruiz, L.A., Hermosilla, T., Mauro, F., Godino, M., 2014. Analysis of the influence of plot size and LiDAR density on forest structure attribute estimates. Forests 5 (5), 936–951.
Singh, K.K., Chen, G., McCarter, J.B., Meentemeyer, R.K., 2015. Effects of LiDAR point density and landscape context on estimates of urban forest biomass. ISPRS J. Photogrammetry and Remote Sens. 101, 310–322. https://doi.org/10.1016/j.isprsjprs.2014.12.021.
Suratno, A., Seielstad, C., Queen, L., 2009. Tree species identification in mixed coniferous forest using airborne laser scanning. ISPRS J. Photogramm. Remote Sens. 64 (6), 683–693.
Valbuena, R., 2015. Forest structure indicators based on tree size inequality and their relationships to airborne laser scanning. Dissertation Forestales 205, 1–87.
Valbuena, R., Packalén, P., Mehtätalo, L., García-Abril, A., Maltamo, M., 2013. Characterizing forest structural types and shelterwood dynamics from Lorenz-based indicators predicted by airborne laser scanning. Can. J. For. Res. 43 (11), 1063–1074.
Valbuena, R., Maltamo, M., Mehtätalo, L., Packalen, P., 2017. Key structural features of Boreal forests may be detected directly using L-moments from airborne lidar data. Remote Sens. Environ. 194, 437–446.
Zhang, G., Peng, H., Zhou, H., Ji, X., Zhang, S., 2022. Comparison of density and basal area estimation of mountain natural forests based on distance-based sampling methods in Zhejiang, China. Ecol. Informat. 68, 101530.